Journal of Scientific Computing (2021) 88:83
https://doi.org/10.1007/s10915-021-01599-5

Calculating Characteristic Roots of Multi-Delayed Systems with Accumulation Points via a Definite Integral Method

Qi Xu[1,2] · Zaihua Wang[3] · Li Cheng[2]

Received: 20 February 2020 / Revised: 1 March 2021 / Accepted: 10 June 2021
© The Author(s), under exclusive licence to Springer Science+Business Media, LLC, part of Springer Nature 2021

Abstract
Multi-delayed systems, especially the neutral ones, have infinitely many and complex distributed characteristic roots that are crucial for system dynamics. The definite integral method, which determines the system stability by using only a definite integral, is extended in this paper for calculating all the characteristic roots in an arbitrarily given area on the complex plane of both retarded and neutral multi-delayed systems with constant discrete delays. Two simple algorithms are proposed for implementing the proposed method, by first calculating the distribution of the real parts of all the characteristic roots, then the imaginary parts by using an iteration method. The real part distribution can be used for the quick estimation of key characteristic roots such as the rightmost ones or the corresponding accumulation point(s), thus allowing adjusting the upper limit of the integral to further simplify the calculation procedure. Examples are given to show the feasibility and the efficiency of the proposed method through numerical analyses.

Keywords Definite integral method · Multi-delay · Neutral time delay differential equation · Characteristic roots · Stability

✉ Li Cheng
li.cheng@polyu.edu.hk

Qi Xu
xuqi@swjtu.edu.cn

Zaihua Wang
zhwang@nuaa.edu.cn

[1] School of Mechanics and Engineering, Southwest Jiaotong University, Chengdu 611756, China

[2] Department of Mechanical Engineering, The Hong Kong Polytechnic University, Hong Kong, China

[3] State Key Lab of Mechanics and Control of Mechanical Structures, Nanjing University of Aeronautics and Astronautics, Nanjing 210016, China

Published online: 07 August 2021

1 Introduction

Time delays are very common in real world, see for instance several engineering applications: Internet control [1], metal cutting [2], man-machine interaction [3], thermo-acoustic interaction [4] and so on [5]. The evolution of a time-delay system depends not only on the present state as in systems described ordinary differential equations (ODEs), but also the past states over previous time period(s). Thus, irrespective of the number of time delays, a time-delay system has always infinite-dimensional solution space. As a matter of fact, time delay often exerts strong impact on system dynamics, such as deteriorating its performance, destabilizing dynamic responses, and results in complex nonlinear behaviors like double Hopf bifurcation [6], chaos [7], and so on [8].

Time-delay systems are usually modeled by delay differential equations (DDEs). Depending on whether the highest-order derivative terms have time delay(s) or not, DDEs can be classified into neutral ones (NDDEs) and retarded ones (RDDEs) [9]. NDDEs have different features compared with RDDEs. For example, in the linear stability analysis that requires the knowledge of root location of the characteristic equation, the infinite number of characteristic roots of an RDDE reside in the left half complex plane of a line parallel to the imaginary axis, while the infinite number of characteristic roots of a linear NDDE are distributed in a strip between two lines that are parallel to the imaginary axis with possible accumulation point(s) on the boundary. Thus, the stability of an RDDE is guaranteed if all the characteristic roots have negative real parts (or equivalently the real part of the rightmost characteristic roots is negative); on the contrary, the stability of an NDDE is ensured if the real part of the rightmost characteristic roots is negative and no accumulation point exists on the imaginary axis. Based on this fact, many stability criteria have been developed for the stability analyses of DDEs, exemplified by the Pontryagin method [10], the Nyquist Plot method [11,12], the Stepan/Hassard method [13,14] and the definite integral method (DIM) [15–17], the linear θ-method [18], all by checking whether the number of characteristic roots with nonnegative real parts is zero. Meanwhile, some algorithms have been proposed for directly calculating the rightmost characteristic roots of some DDEs which also offer means for stability assessment, such as calculating the RDDE's rightmost roots on the basis of the Lambert W function [19], and the NDDE's rightmost roots based on the DIM [20] with strong stability condition [21] holds.

For stable NDDE, whose real part of the rightmost characteristic roots is negative, the stability can be strong or weak, depending on whether the characteristic roots have accumulation point(s) at infinity on the imaginary axis [21]. Strong stability is the case that is most widely investigated in the literature. By comparison, studies on weak stability is relatively scarce. In typical weak stability problems, both the rightmost characteristic roots and the accumulation point(s) are crucial for stability assessment. In addition,as a delay increases from zero to a certain level, the rightmost characteristic roots of DDEs are generated differently from the root branches initiated, either from the rightmost ones of the corresponding delay-free system for short delay, or from other roots of the delay-free system for large delay [4]. This means that other characteristic roots but the rightmost ones might be crucial to the stability of DDEs from a parametric point of view. On the other hand, due to infinity and complex distribution of the characteristic roots of NDDEs, it is not possible to calculate all the characteristic roots whose right part is larger than a given value, if this value is less than the real part of NDDE's accumulation point(s). Thus, an effective algorithm for calculating characteristic roots in a given region of the complex plane is necessary of the stability analysis of NDDEs. There has been a few numerical methods that are able to achieve this for both RDDEs and NDDEs.

As typical examples, the MATLAB package DDE-Biftool [22,23] uses the linear multistep method to discretize the system equation for obtaining approximated characteristic roots in a given region and then uses the Newton-Raphson Method to correct the estimated roots. The QPmR algorithm [25] computes the intersection points of the real and imaginary parts on the meshed complex plane. The advanced QPmP algorithm [26,27] uses the Argument principle to judge the existence of the characteristic roots in a given strip of the complex plane, which enhances the computation efficiency by omitting grids in this strip.

The main objective of this paper is to extend the DIM for calculating the characteristic roots of both RDDEs and NDDEs with constant discrete delays in a given area in the complex plane. Compared with the original DIM that calculates only the rightmost roots under strong stability condition, the currently proposed extended version is applicable to all systems regardless whether the strong stability condition holds or not. To the best of our understanding, the proposed algorithm shows some merits over the existing methods. For example, the definite integral used in the proposed algorithm takes integer jumpings only, and its calculation allows a round error between -0.5 and 0.5, unlike the calculation of real/imaginary numbers using other methods that might be sensitive to the parameter uncertainties. Meanwhile, the extended DIM first gives the distribution of the real parts of the characteristic roots by searching where the calculated number of roots jumps, then finds the imaginary roots by iteration methods. The pre-calculation of the real part distribution is efficient for system analysis. For example, by adjusting the upper limit of the integral, the extended DIM offers a fast way of estimating the rightmost roots and the accumulation point(s), other than estimating them after calculating all the characteristic roots in the given region.

The rest of the paper is organized as follows. Section 2 gives a brief introduction of the original DIM for stability test of both linear RDDEs and NDDEs with constant discrete delays, alongside its application in calculating the rightmost characteristic roots. Section 3 presents the proposed DIM for the calculation the characteristic roots in an arbitrary but bounded area in the complex plane. Then in Sect. 4, four numerical examples of different type of DDEs are illustrated. Finally, in Sect. 5, concluding remarks are summarized.

2 Calculating Rightmost Roots of NDDEs

Consider a linear time invariant delay differential equations (DDE), which takes the form of

$$\dot{x}(t) + \sum_{i=1}^{m} N_i \dot{x}(t-\tau_i) = Ax(t) + \sum_{i=1}^{m} B_i x(t-\tau_i) \tag{1}$$

where $x \in \mathbb{R}^n$, $\tau_i > 0$, A, B_i, $N_i \in \mathbb{R}^{n\times n}$. When $N_k = 0$ for all $k = 1, 2, \ldots, m$, Eq. (1) is referred to as a retarded delay differential equation (RDDE), and when at least one $N_k \neq 0$ for some $k = 1, 2, \ldots, m$, it is called a neutral delay differential equation (NDDE). The characteristic equation of Eq. (1) is in the form of $f(\lambda) = 0$, where $f(\lambda)$ is called the characteristic function which satisfies

$$f(\lambda) = \lambda^n + \sum_{i=0}^{n} \alpha_i(\mathrm{e}^{-\lambda\tau_1}, \ldots, \mathrm{e}^{-\lambda\tau_m})\lambda^{n-i}, \tag{2}$$

where $\alpha_i(z_1, \ldots, z_m)$, $(i = 0, 1, \ldots, n)$, are real polynomials with respect to $z_1 = \mathrm{e}^{-\lambda\tau_1}, \ldots, z_m = \mathrm{e}^{-\lambda\tau_m}$.

From [9], it is proved that the largest real part of the accumulation point(s) of the characteristic roots of system (1), i.e., the value that separates apart the rightmost and non-rightmost

roots, is the largest real part of the roots of

$$1 + \alpha_0(\mathrm{e}^{-\lambda\tau_1}, ..., \mathrm{e}^{-\lambda\tau_m}) = 0\,.$$

The DIM, capable of analyzing the stability of system (1), can also be used to calculate all its rightmost characteristic roots. Next we first introduce the stability criterion by using the DIM.

2.1 Definite Integral Method for Stability Test

The trivial solution $x = 0$ of system (1) is asymptotically stable if and only if all the characteristic roots have negative real parts and are uniformly bounded away from the imaginary axis [8]. To guarantee that the accumulation point(s) of the characteristic roots have negative real parts and are bounded away from the imaginary axis, the strong stability condition stipulates that the coefficient $\alpha_0(\mathrm{e}^{-\lambda\tau_1}, \ldots, \mathrm{e}^{-\lambda\tau_m})$ should satisfy

$$\sup_{\Re(\lambda) > 0,\ |\lambda| \to \infty} \left|\alpha_0(\mathrm{e}^{-\lambda\tau_1}, \ldots, \mathrm{e}^{-\lambda\tau_m})\right| < 1\,. \tag{3}$$

Condition (3) actually guarantees that the roots of $1 + \alpha_0(\mathrm{e}^{-\lambda\tau_1}, \ldots, \mathrm{e}^{-\lambda\tau_m}) = 0$ have negative real parts and are bounded away from the imaginary axis. For single delay cases, if condition (3) does not hold, the system is unstable because the accumulation point(s) has/have positive real part; however in rare cases where multiple time delays exist and are rationally dependent with each other, even if condition (3) does not hold, the accumulation point(s) can still have negative real part(s) and be bounded away from the imaginary axis and the system response of Eq. (1) can be asymptotically stable . This is called weak stability because it is not robust, as an arbitrarily small variance of time delay, which breaks the rational dependence between the time delays, can make the system asymptotically unstable [21].

Lemma 1 *Assuming that the characteristic equation (2) has no roots on the imaginary axis, and condition (3) holds, then there exists a sufficiently large positive real number T_0, such that for all $T \geq T_0$, the integer number $\mathcal{N}$ of the unstable characteristic roots, i.e., the roots whose real parts are positive, is located in the interval*

$$\mathcal{N} \in \left(-\frac{F(0,T)}{\pi} + \frac{n-1}{2}, -\frac{F(0,T)}{\pi} + \frac{n+1}{2}\right)\,, \tag{4}$$

where

$$F(0,T) = \int_0^T \Re\left(\frac{f'(\mathrm{i}\omega)}{f(\mathrm{i}\omega)}\right)\mathrm{d}\omega \tag{5}$$

with $\Re(z)$ denoting the real part of a complex number z.

Lemma 1 suggests that the exact number $\mathcal{N}$ of the unstable characteristic roots of an NDDE satisfying condition (3) can be easily calculated by rounding off

$$\mathcal{N} = \mathrm{round}\left(\frac{n}{2} - \frac{F(0,T)}{\pi}\right)\,.$$

If $\mathcal{N} = 0$, the corresponding NDDE must be asymptotically stable.

2.2 Calculating the Rightmost Characteristic Roots

A direct application of the DIM is to calculate the rightmost characteristic roots of system (1):

Lemma 2 *Assuming that the strong stability condition holds for $f(\lambda+\delta)=0$, and no roots of $f(\lambda+\delta)=0$ are on the imaginary axis, there exists a sufficiently large positive real number T_0, such that for all $T \geq T_0$ one has*

$$\mathcal{N}(\delta) = \text{round}\left(\frac{n}{2} - \frac{1}{\pi}\int_0^T \Re\left(\frac{f'(\delta+\omega\,\mathrm{i})}{f(\delta+\omega\,\mathrm{i})}\right)\mathrm{d}\omega\right).$$

Remark 1 The roots of $f(\lambda+\delta)=0$ are the same as the roots of $f(\lambda)=0$ but shifted δ leftward in the complex plane. Thus using Lemma 2, when δ keeps decreasing from a large value δ_0 which guarantees that all the real parts of the roots of $f(\lambda)=0$ are less than δ_0, it can be proved that $\mathcal{N}(\delta)$ increases from 0 to infinity. Meanwhile $\mathcal{N}(\delta)$ jumps at δ when δ is the real part of at least one of the roots of $f(\lambda)=0$. Upon getting the root's real part, the imaginary part can be easily carried out by using iteration method.

It is worth noting that the exploration of the characteristic roots is an elaborated way to analyze stability boundaries. For certain complex systems, however, the characteristic functions can be hard to compute and numerical perturbations of system parameters can affect the robustness of the characteristic root calculation as well as the stability assessment, especially for NDDEs when time delays are perturbed. For these complex systems, other stability methods directly based on the system equation may be utilized.

Remark 2 For an RDDE, $\mathcal{N}(\delta)$ goes to infinity only when δ goes to negative infinity, thus all the roots in a bounded area can be calculated. However for an NDDE, $\mathcal{N}(\delta)$ goes to infinity when δ approaches the real part of the accumulation point(s), and all the roots whose real part are smaller than the real part of the accumulation points, can not be calculated using Lemma 2.

3 Calculating Characteristic Roots Located in a Bounded Area

This section aims at improving the DIM, so as to calculate the characteristic roots of system (1) in any bounded area in the complex plane, without imposing the strong stability condition (3).

A general relationship between the integral (5) and the number of the unstable roots $\mathcal{N}$ can be obtained from the Argument Principle:

Lemma 3 *For delay differential system (1), assuming that the characteristic equation $f(\lambda)=0$ has no roots on the boundary of Curves C_1 and C_2, as shown in Fig. 1, and let $\mathcal{N}$ be the number of all the characteristic roots of Eq. (2) in the area encircled by C_1 and C_2, one has*

$$\mathcal{N} = \frac{n}{2} - \frac{F(0,R)}{\pi} + A(R) \tag{6}$$

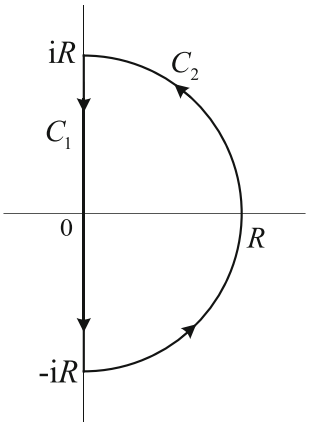

Fig. 1 Contour C_1 and C_2

where,

$$A(R) = \frac{1}{2\pi}\arg\left(1+\sum_{i=0}^{n}\frac{\alpha_i(\mathrm{e}^{-\mathrm{i}R\tau_1},\ldots,\mathrm{e}^{-\mathrm{i}R\tau_m})}{(\mathrm{i}R)^i}\right) - \frac{1}{2\pi}\arg\left(1+\sum_{i=0}^{n}\frac{\alpha_i(\mathrm{e}^{\mathrm{i}R\tau_1},\ldots,\mathrm{e}^{\mathrm{i}R\tau_m})}{(-\mathrm{i}R)^i}\right)$$

Proof Directly from Argument Principle, one has that

$$\begin{aligned}\mathcal{N} &= \frac{1}{2\pi}\Delta_C\arg(f(\lambda)) \\ &= \frac{1}{2\pi}\left(\Delta_{C_1}\arg(f(\lambda)) + \Delta_{C_2}\arg(f(\lambda))\right)\end{aligned} \tag{7}$$

Calculate $\Delta_{C_1}\arg(f(\lambda))$, from $\{\lambda = \mathrm{i}\omega |\ \omega \in (-R,\ R)\}$ one has

$$\Delta_{C_1}\arg(f(\lambda)) = \arg(f(\mathrm{i}\omega))\Big|_{\omega=R}^{\omega=-R} = -2\arg(f(\mathrm{i}\omega))\Big|_{\omega=0}^{\omega=R}.$$

It is easy to prove that [16]

$$\frac{\mathrm{d}}{\mathrm{d}\omega}\arg(f(\mathrm{i}\omega)) = \Re\left(\frac{f'(\mathrm{i}\omega)}{f(\mathrm{i}\omega)}\right)$$

therefore one has

$$\Delta_{C_1}\arg(f(\lambda)) = -2\int_0^R \Re\left(\frac{f'(\mathrm{i}\omega)}{f(\mathrm{i}\omega)}\right)\mathrm{d}\omega = -2F(0,\ R)\,. \tag{8}$$

Calculating $\Delta_{C_2}\arg(f(\lambda))$ yields

$$\begin{aligned}\Delta_{C_2}\arg(f(\lambda)) &= \Delta_{C_1}\arg\left(\lambda^n\left(1+\sum_{i=0}^{n}\frac{\alpha_i(\mathrm{e}^{-\mathrm{i}R\tau_1},\ldots,\mathrm{e}^{-\mathrm{i}R\tau_m})}{\lambda^i}\right)\right) \\ &= \Delta_{C_2}\arg(\lambda^n) + \Delta_{C_1}\arg\left(1+\sum_{i=0}^{n}\frac{\alpha_i(\mathrm{e}^{-\mathrm{i}R\tau_1},\ldots,\mathrm{e}^{-\mathrm{i}R\tau_m})}{\lambda^i}\right),\end{aligned}$$

substituting $\lambda = Re^{i\theta} \mid \theta \in (-\pi/2, \pi/2)\}$ into the above equation generates

$$\begin{aligned}\Delta_{C_2}\arg(f(\lambda)) &= n\frac{\pi}{2} - n\left(-\frac{\pi}{2}\right) + \arg\left(1 + \sum_{i=0}^{n} \frac{\alpha_i(e^{-\tau_1 Re^{\pi i/2}}, \cdots, e^{-\tau_m Re^{\pi i/2}})}{\left(Re^{\pi i/2}\right)^i}\right) \\ &\quad - \arg\left(1 + \sum_{i=0}^{n} \frac{\alpha_i(e^{-\tau_1 Re^{-\pi i/2}}, \ldots, e^{-\tau_m Re^{-\pi i/2}})}{\left(Re^{-\pi i/2}\right)^i}\right) \\ &= n\pi + \arg\left(1 + \sum_{i=0}^{n} \frac{\alpha_i(e^{-iR\tau_1}, \ldots, e^{-iR\tau_m})}{(iR)^i}\right) - \\ &\quad \arg\left(1 + \sum_{i=0}^{n} \frac{\alpha_i(e^{iR\tau_1}, \ldots, e^{iR\tau_m})}{(-iR)^i}\right) \\ &= n\pi + 2\pi A(R)\,.\end{aligned} \tag{9}$$

Equation (6) can be derived from Eqs. (7), (9) and (8). This completes the proof.

Remark 3 Lemma 3 applies to both RDDEs and NDDEs, regardless whether condition (3) holds or not. For RDDEs and strong stability cases of NDDEs, it can be proved that any $|A(R)|$ is strictly less than $1/2$ for a sufficiently large R. Hence Eq. (4) holds, where the critical upper limit T of Eq. (4) is given in [17]. However, for weak stability cases, $A(R)$ can be either bounded or unbounded when R gets larger and larger. Even if bounded, $|A(R)|$ can be either less, equal or even larger than $1/2$: for the larger than $1/2$ case, there are more than one integer that satisfy Eq. (4), only one of which is the right $\mathcal{N}$.

Based on Lemma 3, the following theorem is proposed for the unstable roots of $f(\lambda) = 0$ when they are shifted in the complex plane:

Theorem 1 *Assuming that the characteristic equation $f(\lambda+\delta_0) = 0$ and $f(\lambda+\delta) = 0,\ 0 < |\delta - \delta_0| << 1$ both have no roots on the boundary of Curves C1 and C2, as shown in Figure 1, and letting $\mathcal{N}_{\delta_0}$ and $\mathcal{N}_\circ$ be the number of all the characteristic roots of $f(\lambda) = 0$ and $f(\lambda + \delta) = 0$ in the area encircled by C1 and C2, respectively, for any $\epsilon > 0$, there exists a $\gamma > 0$, such that for $|\delta - \delta_0| < \gamma$,*

$$\mathcal{N}_\delta - \mathcal{N}_{\delta_0} - \epsilon < \frac{F_{\delta_0}(0, R)}{\pi} - \frac{F_\delta(0, R)}{\pi} < \mathcal{N}_\delta - \mathcal{N}_{\delta_0} + \epsilon\,, \tag{10}$$

where

$$F_\delta(0, R) = \int_0^R \Re\left(\frac{f'(i\omega + \delta)}{f(i\omega + \delta)}\right) d\omega\,.$$

Proof Denoting that

$$\begin{aligned}A_\delta(R) &= \frac{1}{2\pi}\arg\left(1 + \sum_{i=0}^{n} \frac{\alpha_i(e^{-(iR+\delta)\tau_1}, \ldots, e^{-(iR+\delta)\tau_m})}{(iR)^i}\right) \\ &\quad - \frac{1}{2\pi}\arg\left(1 + \sum_{i=0}^{n} \frac{\alpha_i(e^{(iR+\delta)\tau_1}, \ldots, e^{(iR+\delta)\tau_m})}{(-iR)^i}\right),\end{aligned}$$

then from Lemma 3, one has

$$\mathcal{N}_\delta = \frac{n}{2} - \frac{F_\delta(0, R)}{\pi} + A_\delta(R)\,.$$

Hence, it yields that

$$\mathcal{N}_\delta - \mathcal{N}_{\delta_0} = \frac{F_{\delta_0}(0, R)}{\pi} - \frac{F_\delta(0, R)}{\pi} + A_\delta(R) - A_{\delta_0}(R), \tag{11}$$

Notice that $\alpha_i(z_1, \ldots, z_m), i = 0, 1, \ldots, n$ are real polynomials with respect to $z_1 = \mathrm{e}^{-\lambda\tau_1}, \ldots, z_m = \mathrm{e}^{-\lambda\tau_m}$ as stated above. Thus for $R > 0$, $A_\delta(R)$ is continuous with respect to $\delta = \delta_0$, which means that for any $\epsilon > 0$, there exists a $\gamma > 0$ such that for $|\delta - \delta_0| < \gamma$

$$\left|A_\delta(R) - A_{\delta_0}(R)\right| < \epsilon. \tag{12}$$

From Eqs. (11) and (12) , one has

$$\mathcal{N}_\delta - \mathcal{N}_{\delta_0} - \epsilon < \frac{F_{\delta_0}(0, R)}{\pi} - \frac{F_\delta(0, R)}{\pi} < \mathcal{N}_\delta - \mathcal{N}_{\delta_0} + \epsilon\ .$$

This completes the proof of Theorem 1.

Remark 4 The value $\mathcal{N}_\delta - \mathcal{N}_{\delta_0}$ is an integer, thus for a small enough δ varying in the neighborhood of δ_0, the characteristic roots of $f(\lambda + \delta_0)$ encircled by $C1$ and $C2$ may become different from that of $f(\lambda + \delta)$, which indicates that $\mathcal{N}_\delta - \mathcal{N}_{\delta_0}$ will jump to a certain integer. Consequently, Theorem 1 stipulates that the value of $\frac{F_{\delta_0}(0,R)}{\pi} - \frac{F_\delta(0,R)}{\pi}$ will also jump a value close to this integer. As in the case of $\mathcal{N}_\delta - \mathcal{N}_{\delta_0} = 0$, the value of $\frac{F_{\delta_0}(0,R)}{\pi} - \frac{F_\delta(0,R)}{\pi}$ remains in a small neighborhood of 0.

The exact relationship between the roots of $f(\lambda) = 0$ and the jumping of $\mathcal{N}_\delta$ is as follows:

Theorem 2 *As δ is increasing in a small enough neighborhood of δ_0, calculating the two values of $\mathcal{N}_\delta$ when $\delta = \delta_0^+$ and $\delta = \delta_0^-$, if $\mathcal{N}_{\delta_0^+} - \mathcal{N}_{\delta_0^-}$ decreases, then δ_0 is the real part of at least one of the roots of $f(\lambda) = 0$. Moreover, defining $\Delta_N = \mathcal{N}_{\delta_0^-} - \mathcal{N}_{\delta_0^+}$ (positive means decrease case and negative increase case) and denoting the exact number of roots of $f(\lambda) = 0$ whose real part is δ_0 by N_{δ_0}, one has $\Delta_N \le N_{\delta_0}$.*

Proof When δ is increasing in a small enough neighborhood of $\delta = \delta_0$, all the roots of $f(\lambda + \delta) = 0$ are shifted rightward in the complex plane. Four cases corresponding to the root shifting leftward are illustrated in Fig. 2 and discussed below.

Case 1. No roots are crossing C_1 and C_2, as shown in Fig. 2b. Thus $N_{\delta_0} = 0$. Noticing that $\mathcal{N}_\delta$ is the number of characteristic roots of $f(\lambda + \delta)$ encircled by C_1 and C_2, thus $\Delta_N = \mathcal{N}_{\delta_0^-} - \mathcal{N}_{\delta_0^+} = 0$, and hence $\Delta_N = 0 = N_{\delta_0}$.

Case 2. There is at least one root that is crossing C_1 and no root is crossing C_2, as shown in Fig. 2b. In this case $\mathcal{N}_{\delta_0^+} - \mathcal{N}_{\delta_0^-}$ decreases, and there are Δ_N number of roots shifting out of the region encircled by C_1 and C_2, where δ_0 corresponds to the critical situation that there is/are Δ_N number of root(s) located on C_1. Hence, there are Δ_N number of roots of $f(\lambda + \delta_0) = 0$ whose real part is 0, i.e., Δ_N number of roots of $f(\lambda) = 0$ whose real part is $\Re(\lambda) = \delta_0$. Hence, $0 < \Delta_N = N_{\delta_0}$.

Case 3. There is at least one root that is crossing C_2 and no root is crossing C_1, as shown in Fig. 2c, thus $N_{\delta_0} = 0$. Similarly to Case 2, it can be proved that $\mathcal{N}_{\delta_0^+} - \mathcal{N}_{\delta_0^-}$ increases. and $\delta = \delta_0$ corresponds to the critical situation that for $f(\lambda + \delta_0) = 0$, there are $-\Delta_N$ number of roots located on C_2. Hence $\Delta_N < N_{\delta_0} = 0$

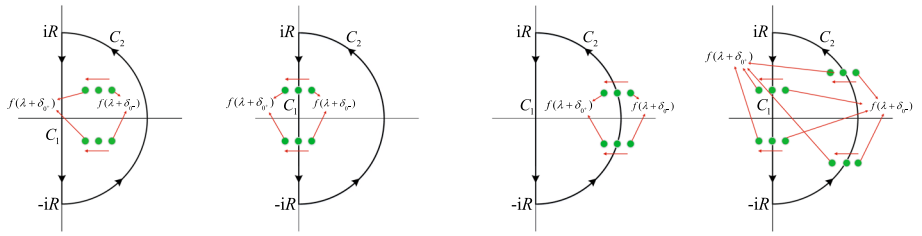

Fig. 2 The root tendency of **a**: Case 1; **b**: Case 2; **c**: Case 3; and **d**: Case4

Case 4. There are roots crossing both C_1 and C_2 at the same time, as shown in Fig. 2d. In this case, $\mathcal{N}_{\delta_0^+} - \mathcal{N}_{\delta_0^-}$ may either decrease, stay the same, or increase, depending on whether the number of roots of $f(\lambda) = 0$ on C_1 is more than, equal to, or less than that of C_2. And respectively, one has $0 < \Delta_N < N_{\delta_0}$, $\Delta_N = 0 < N_{\delta_0}$, or $\Delta_N < 0 < N_{\delta_0}$.

For all above cases, it can be seen that $\Delta_N > 0$ always relates to the cases where δ_0 is the real part of at least one of the roots of $f(\lambda) = 0$, and for all cases one has $\Delta_N < N_{\delta_0}$. This completes the proof.

Remark 5 The condition $\Delta_N > 0$ is only a necessary one for the cases where δ_0 is the real part of at least one of the roots of $f(\lambda) = 0$. As can be seen from Case 4 that, $\Delta_N \geq 0$ can relates to that δ_0 is the real part of at least one of the roots of $f(\lambda) = 0$. However, Case 4 is rare and can be easily avoided by choosing a different radius R for the contour C_1 and C_2. This R must exist, since the characteristic roots of $f(\lambda) = 0$ in a bounded contour C_1 and C_2 is always limited, and one can always find a bounded contour for which Case 4 will not happen by shifting all these limited roots.

Corollary 1 *Assuming that the radius R for contour C_1 and C_2 is properly chosen such that Case 4 does not happen, hence for small enough δ varying in the neighborhood of δ_0, one has that, $f(\lambda) = 0$ has root(s) whose real part is $\Re(\lambda) = \delta_0$ if and only if*

$$\text{round}\left(\frac{F_{\delta_0^-}(0, R)}{\pi} - \frac{F_{\delta_0^+}(0, R)}{\pi}\right) < 0\,.$$

Moreover, the number of these roots N_{δ_0} satisfies

$$N_{\delta_0} = \text{round}\left(\frac{F_{\delta_0^+}(0, R)}{\pi} - \frac{F_{\delta_0^-}(0, R)}{\pi}\right)\,. \tag{13}$$

Proof From Theorem 1, by choosing $\epsilon = 1/2$, one has

$$\text{round}\left(\frac{F_{\delta_0^-}(0, R)}{\pi} - \frac{F_{\delta_0^+}(0, R)}{\pi}\right) = \mathcal{N}_{\delta_0^+} - \mathcal{N}_{\delta_0^-}\,.$$

The condition $\mathcal{N}_{\delta_0^+} - \mathcal{N}_{\delta_0^-} = -\Delta_N < 0$ with properly chosen contour radius R, satisfies Case 2, then from Theorem 2 one has that $N_{\delta_0} = \Delta_N$, which completes the proof.

Algorithm 1 Based on Corollary 1, the following algorithm can be compiled to calculate the roots in a bounded square region $\{(a, b) \times (-R\text{i}, R\text{i}) \mid a, b, R \in \mathbb{R}\}$:

Step 1. Calculate the characteristic function $f(\lambda)$ in Eq. (2).
Step 2. Choose a sufficiently small number $\delta > 0$, vary δ_0 in a meshed (a, b), and calculate

$$\text{round}\left(\frac{F_{\delta_0^-}(0,R)}{\pi} - \frac{F_{\delta_0^+}(0,R)}{\pi}\right) = \text{round}\int_0^R \left[\Re\left(\frac{f'(\mathrm{i}\omega+\delta_0-\delta)}{f(\mathrm{i}\omega+\delta_0-\delta)}\right) - \Re\left(\frac{f'(\mathrm{i}\omega+\delta_0+\delta)}{f(\mathrm{i}\omega+\delta_0+\delta)}\right)\right]\mathrm{d}\omega\,.$$

Step 3. If the calculated value in Step 2 decreases at $\delta_0 = \sigma_0$, then the characteristic root(s) of $f(\lambda) = 0$ can be obtained numerically with the estimation $\lambda_0 = \sigma_0 + \mathrm{i}\omega_0$, $\omega_0 < R$, by using the Newton-Raphson iteration method within a few iterations steps [16]:

$$\lambda_{i+1} = \lambda_i - \frac{f(\lambda_i)}{f'(\lambda_i)}, \quad i = 0, 1, 2, \ldots \tag{14}$$

In practice, Step 2 will most likely yield value of 0 in most cases, whilst only in limited cases it yields none zero values. Also, if δ is too small while the meshed δ_0 is not small enough, the values following Step 2 would be all 0 for the meshed δ_0, which deteriorates the applicability of Algorithm 1.

The following theorem is the main result of the paper.

Theorem 3 *With the condition of corollary 1, and assuming that* $\frac{F_{\delta_0^+}(0,R)}{\pi} \neq k + 1/2, k \in \mathbb{Z}$, *then for small enough* δ *varying in the neighborhood of* δ_0, $f(\lambda) = 0$ *has root(s) whose real part is* $\Re(\lambda) = \delta_0$ *if and only if*

$$\text{round}\left(\frac{F_{\delta_0^-}(0,R)}{\pi}\right) - \text{round}\left(\frac{F_{\delta_0^+}(0,R)}{\pi}\right) < 0\,.$$

Moreover, the number of these roots N_{δ_0} *satisfies*

$$N_{\delta_0} = \text{round}\left(\frac{F_{\delta_0^-}(0,R)}{\pi}\right) - \text{round}\left(\frac{F_{\delta_0^+}(0,R)}{\pi}\right)\,. \tag{15}$$

Proof Let $\frac{F_{\delta_0^+}(0,R)}{\pi} = k + \gamma$, $-1/2 < \gamma < 1/2$, which suggests

$$\text{round}\left(\frac{F_{\delta_0^+}(0,R)}{\pi}\right) = k. \tag{16}$$

Then from Theorem 1, one has

$$\frac{F_{\delta_0^+}(0,R)}{\pi} + \mathcal{N}_{\delta_0^+} - \mathcal{N}_{\delta_0^-} - \epsilon < \frac{F_{\delta_0^-}(0,R)}{\pi} < \frac{F_{\delta_0^+}(0,R)}{\pi} + \mathcal{N}_{\delta_0^+} - \mathcal{N}_{\delta_0^-} + \epsilon\,.$$

For the case of $0 \le \gamma < 1/2$, by choosing $0 < \epsilon < 1/2 - \gamma$, it yields

$$k + \mathcal{N}_{\delta_0^+} - \mathcal{N}_{\delta_0^-} + 2\gamma - 1/2 < \frac{F_{\delta_0^-}(0,R)}{\pi} < k + \mathcal{N}_{\delta_0^+} - \mathcal{N}_{\delta_0^-} + 1/2\,,$$

which is equivalent to

$$k + \mathcal{N}_{\delta_0^+} - \mathcal{N}_{\delta_0^-} - 1/2 < \frac{F_{\delta_0^-}(0,R)}{\pi} < k + \mathcal{N}_{\delta_0^+} - \mathcal{N}_{\delta_0^-} + 1/2\,.$$

Same result can be obtained for the case of $-1/2 < \gamma < 0$ by choosing $0 < \epsilon < \gamma + 1/2$. Thus for $-1/2 < \gamma < 1/2$, one has

$$\text{round}\left(\frac{F_{\delta_0^-}(0,\,R)}{\pi}\right) = k + \mathcal{N}_{\delta_0^+} - \mathcal{N}_{\delta_0^-}. \tag{17}$$

Equations (16) and (17) give

$$\mathcal{N}_{\delta_0^+} - \mathcal{N}_{\delta_0^-} = \text{round}\left(\frac{F_{\delta_0^-}(0,\,R)}{\pi}\right) - \text{round}\left(\frac{F_{\delta_0^+}(0,\,R)}{\pi}\right)$$

Same as Corollary 1, the condition $\mathcal{N}_{\delta_0^+} - \mathcal{N}_{\delta_0^-} < 0$ satisfies Case 2, and the conclusion can be proved similarly.

Different from Eq. (13) in Corollary 1, the right hand side of Eq. (15) indicates that in practice, the real-part-distribution of the roots of $f(\lambda) = 0$ in $\{(a, b) \times (-R\mathrm{i},\, R\mathrm{i}) \mid a, b, R \in \mathbb{R}\}$ can be identified by just calculating

$$\text{round}\left(\frac{F_\delta(0,\,R)}{\pi}\right) = \text{round}\left(\frac{1}{\pi}\int_0^R \Re\left(\frac{f'(\mathrm{i}\omega+\delta)}{f(\mathrm{i}\omega+\delta)}\right)\mathrm{d}\omega\right) \tag{18}$$

with δ varies in the meshed (a, b). More precisely, as δ increases in the neighborhood of $\delta = \sigma_0$, if the calculated value of Eq. (18) jumps from one integer k_1 to a larger integer k_2, one can conclude that the number of roots of $f(\lambda) = 0$ with the real part $\Re(\lambda) \approx \sigma_0$ is equal to $k_2 - k_1$. Thus, we call the jumps of value of Eq. (18) as root jump in the following.

Thus, a simpler and more practical **Algorithm 2** can be proposed, by revising Step 2 and Step 3 in Algorithm 1 as:
Step 2. Vary δ in a meshed (a, b), and calculate the value as expressed in Eq. (18).
Step 3. If root jump happens, i.e., the calculated value of Eq. (18) jumps to larger integer as δ increases in the neighborhood of $\delta = \sigma_0$, then the characteristic root(s) of $f(\lambda) = 0$ can be obtained similarly as that of Step 3 in Algorithm 1.

Remark 6 Both Algorithm 1 and 2 need a properly chosen radius R of contour C_1 and C_2 to avoid Case 4. In practice, Algorithm 2 is recommended for use, and a randomly chosen R usually can satisfy the needed condition, since the number of roots of $f(\lambda) = 0$ is limited for bounded R. Also, repeating the procedures of Algorithm 2 by choosing two different R, and if the jumping remains the same, this would further increase the reliability of the results.

Remark 7 If condition $\frac{F_{\delta_0^+}(0,R)}{\pi} \neq k + 1/2, k \in \mathbb{Z}$ does not hold, Eq. (18) may increase even when the number of roots does not change. This false increment is exactly 1 while usually the corresponding increment is 2 when the number of roots does change, as shown in Case 2. Similarly as Remark 6, repeating the procedures of Algorithm 2 by choosing two different R would help to identify the false increment.

Remark 8 Condition $\frac{F_{\delta_0^+}(0,R)}{\pi} = k + 1/2, k \in \mathbb{Z}$ introduces discontinuity to the rounding off value of $F_\delta(0,\,R)/\pi$ in the neighborhood of $\delta = \delta_0$. However, it does not affect the continuity of the value of $F_\delta(0,\,R)/\pi$ in the neighborhood of $\delta = \delta_0$. Hence, the false increment caused by $\frac{F_{\delta_0^+}(0,R)}{\pi} = k + 1/2, k \in \mathbb{Z}$ can be avoided by using just $F_\delta(0,\,R)/\pi$ instead of rounding it off. In this case, a root jump only happens when $F_\delta(0,\,R)/\pi$ jumps.

It is worth noting that popular tools like DDE-Biftool and QPmR (including the advanced QPmR) carry out the stability analysis of time-delay systems also through calculating the

characteristic roots. The extended DIM provides an alternative way of doing this, and it shows some merits over the existing methods. For example, the definite integral used in the extended DIM only takes integer values or integer jumps, and its calculation allows a round error between -0.5 and 0.5. As a result, the proposed algorithm is expected to be less sensitive to the parameter uncertainties. Meanwhile, the advanced QPmR method calculates the characteristic roots in a similar way as the extended DIM following Algorithm 2: it first judges the existence of the characteristic roots in a given strip of the complex plane by directly employing Argument Principle, and then calculates the characteristic roots in grids by using the original QPmR method while omitting the strips that have no characteristic roots. The first step of the argument calculation of the advanced QPmR method is converted into a closed curve integral over a square strip with four different sides, while the extended DIM, based also on Argument Principle, calculates a closed curve integral with the same integrand over a half circle and further simplifies this closed curve integral into a simple definite integral. Thus the definite integral method could be more computational efficient and easily programmed compared to the advanced QPmR method for argument calculation.

4 Numerical Illustrations

Example 1 As the first example, we calculate the roots of an RDDE which takes the form of

$$\dot{x}(t) + ax(t) + bx(x-1) = 0 \tag{19}$$

As stated in Example (3.25) in [13], system (19) is unstable for $a = -0.5, b = 1$. From Eq. (2), the characteristic function when $a = -0.5, b = 1$ takes the form of

$$f(\lambda) = \lambda - 0.5 + \mathrm{e}^{-\lambda}$$

Since the system is unstable, it must have root(s) whose real part is positive. However, in this example, we are interested in calculating the roots with negative real parts that locate in the square $(-10, 0) \times (-200\mathrm{i}, 200\mathrm{i})$ in the complex plane.

Directly applying Algorithm 2 for $R = 100$, the real-part-distribution can be clearly identified from Fig. 3.

Following Step 2, root jump happens 16 times, i.e., the calculated value round $\left(\frac{F_\delta(0,R)}{\pi}\right)$ increases 16 times, and each time the increment is 2, which means there are totally 16 pairs of conjugate roots of $f(\lambda) = 0$ located in the square region $(-10, 0) \times (-200\mathrm{i}, 200\mathrm{i})$, and the real parts of these roots are the coordinates where jumping takes place.

Then following Step 3, further calculating by using the Newton-Raphson iteration method can give the approximated value of all these roots, among which the left most 3 pairs are $-4.563 \pm 95.768\mathrm{i}$,$-4.496 \pm 89.480\mathrm{i}$ and $-4.260 \pm 70.619\mathrm{i}$, and the rightmost 3 pairs are $-2.658 \pm 13.914\mathrm{i}$,$-2.073 \pm 7.524\mathrm{i}$, $-0.163 \pm 0.972\mathrm{i}$.

Example 2 In this example, we calculate the roots of a multi-delay NDDE for which the strong stability condition (3) holds [28]:

$$\ddot{z}(t) + 2\zeta_1\dot{z}(t) + z(t) + p\ddot{z}(t-\tau_1) + 2\zeta_2\dot{z}(t-\tau_2) = 0\,, \tag{20}$$

where $p = 0.4, \xi_1 = 0.25, \xi_2 = 0.24$ and the two delay values are $\tau_1 = 4, \tau_2 = 3$. The characteristic function reads as

$$f(\lambda) = (1 + 0.4\,\mathrm{e}^{-4\lambda})\lambda^2 + (0.5 + 0.48\mathrm{e}^{-3\lambda})\lambda + 1. \tag{21}$$

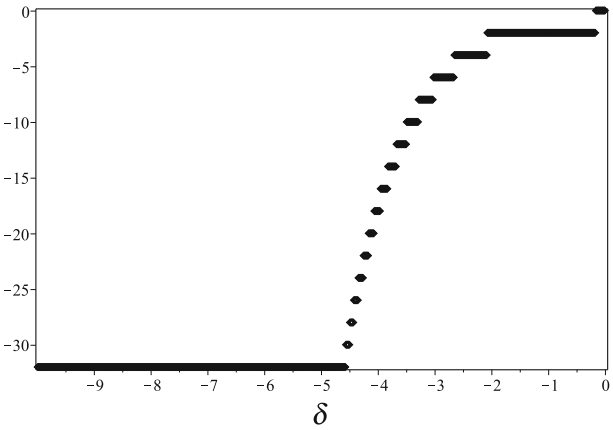

Fig. 3 Root jump with respect to δ in $(-100,0)$ when $R = 100$ for system (19)

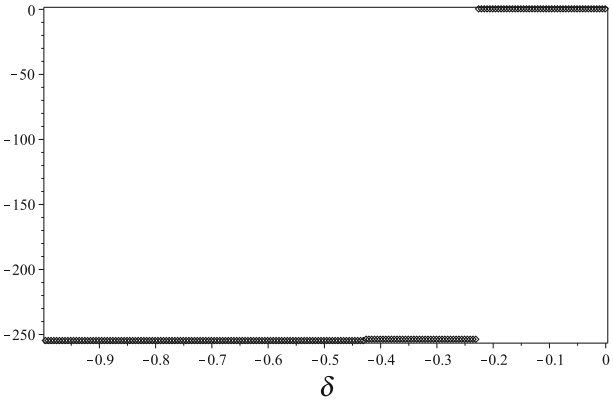

Fig. 4 Root jump with respect to $\delta \in (-1, 0)$ when $R = 200$ for Eq. (22)

The rightmost and non-rightmost roots are divided by the infinitely many roots of

$$1 + 0.4\mathrm{e}^{-4\lambda} = 0\,, \tag{22}$$

which is an NDDE with one single delay. The roots of Eq. (22) can be theoretically calculated as

$$\lambda_0 = -\frac{1}{4}\ln\left(\frac{5}{2}\right) - \frac{1}{4}(1+2k)\pi\mathrm{i},\ k = 1, 2, \ldots$$

Notice that the number of the roots of Eq. (22) is infinitely many, and all the roots share the identical real part $\Re(\lambda_0) \approx -0.229$ with the imaginary part goes to infinity. Thus it can be proved that for system (20), there are infinitely many roots of Eq. (21) whose the real parts approaches to $\Re(\lambda_0)$ while the imaginary part goes to infinity, and $\Re(\lambda_0)$ distinguishes the rightmost roots and the non-rightmost roots of Eq. (21) [9].

Since Eq. (22) is an NDDE, the proposed extended version of DIM can also be applied. By applying $\delta \in (-1, 0)$ and $R = 100$, the results from Step 2 are plotted for the roots of Eq. (22) in $(-1, 1) \times (-200\mathrm{i}, 200\mathrm{i})$ as shown in Fig. 4, from which we can see that the value jumps over 250 at $\delta \approx -0.229$. This indicates that at least more than 250 roots of Eq. (22)

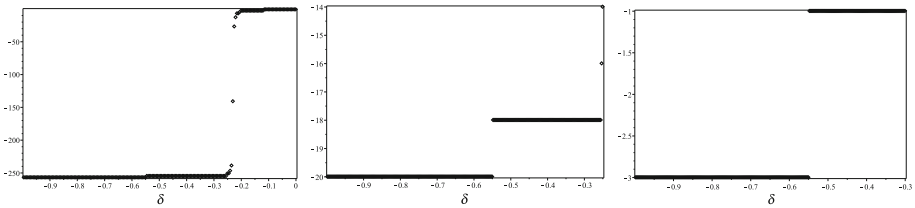

(a) (b) (c)

Fig. 5 Root jump with respect to **a**: $\delta \in (-1, 0)$, $R = 100$; **b**: $\delta \in (-1, -0.25)$, $R = 10$ and **c**: $\delta \in (-1, -0.3)$, $R = 10$ for Eq. (21)

are located in $(-1, 1) \times (-200\mathrm{i}, 200\mathrm{i})$, with their real parts being close to -0.229. Hence, a good guess can be made that there are infinitely many roots of Eq. (22) whose real part is close to -0.229, and the rightmost roots should be those whose real parts are larger than -0.229.

Next, we calculate all the roots of Eq. (22) located in the square $(-1, 1) \times (-200\mathrm{i}, 200\mathrm{i})$ of the complex plane, as well as the non-rightmost roots in the square $(-1, -0.25) \times (-10\mathrm{i}, 10\mathrm{i})$ and the square $(-1, -0.3) \times (-2\mathrm{i}, 2\mathrm{i})$. Applying Algorithm 2 for $\delta \in (-1, 0)$, $R = 100$; $\delta \in (-1, -0.3)$, $R = 10$ and $\delta \in (-1, -0.3)$, $R = 10$, respectively. The calculated results from Step 2 are plotted in Fig. 5a, b, c.

From Fig. 5a, it can be seen that root jump happens many times, and the increment around $\delta \approx -0.229$ is the highest, which suggests that the accumulation point of Eq. (20) is around $\delta \approx -0.23$. Together with Fig. 4, both figures increase rapidly at $\delta \approx -0.23$, which testifies that both Eq. (21) and Eq. (22) have the same accumulation points.

From Fig. 5b, it can be seen that root jump value increases 2 by three times, one at $\delta \approx -0.55$ and the other two at $\delta \approx -0.25$. Then from Fig. 5c the root jump value increases 2 by only once, at $\delta \approx -0.55$. Comparing these two figures, one can conclude that the imaginary part of the conjugate roots corresponding to $\delta \approx -0.55$ must be $-3 < \omega < 3$, and the other two pairs of conjugate roots corresponding to $-15 < \omega < -3$, or $3 < \omega < 15$. From Step 3, the approximated values of all these roots are calculated as $-0.550 \pm 0.255\mathrm{i}$, $-0.250 \pm 4.006\mathrm{i}$ and $-0.252 \pm 5.488\mathrm{i}$, which agrees with the analysis from both Figs. 5b and c.

Example 3 This example considers a special NDDE, which has only non-rightmost roots and does not satisfy the strong stability condition. The system equation takes the form of [20]

$$\dot{x}(t) + p\dot{x}(t - \tau) + ax(t) = 0\,, \tag{23}$$

where $p = 1, a = 0.5, \tau = 0.3$. The characteristic function reads as

$$\left(1 + \mathrm{e}^{-0.3\lambda}\right)\lambda + 0.5 = 0. \tag{24}$$

It has been proved in [20] that all the roots of Eq. (23) are non-rightmost ones, whose accumulation point's real part is 0. With the proposed method, we evaluate the roots in the square $(-0.002, 0.001) \times (-R\mathrm{i}, R\mathrm{i})$ for $R = 2000$ or $R = 100$, and give the real part distribution based on Step 2 of Algorithm 2. It can be seen from Fig. 6a that, more than 90 roots are located in $(-0.002, 0.001) \times (-2000\mathrm{i}, 2000\mathrm{i})$, and all of them have negative real parts which are very close to zero. Thus it could be concluded that the accumulation point's real part is approximately zero. In addition, the values in Fig. 6a jump rapidly for $\delta < 0$ while keeping invariant for $\delta > 0$, this suggests that there are no roots whose real parts are

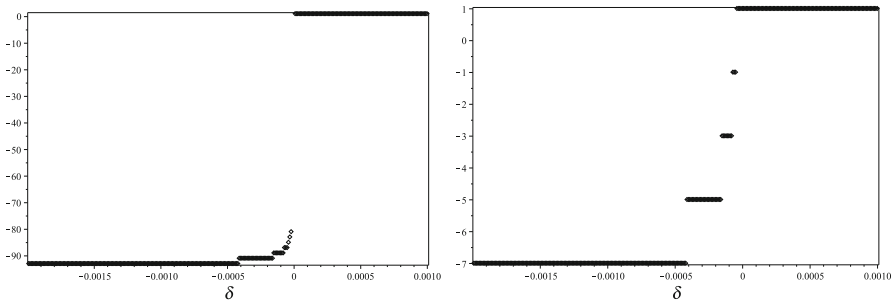

Fig. 6 Root jump with respect to $\delta \in (-0.002, 0.001)$ with **a**: $R = 2000$ and **b**: $R = 100$, for system (23)

positive, i.e., no rightmost roots, exist in $(-0.002, 0.001) \times (-2000\mathrm{i}, 2000\mathrm{i})$. In Fig. 6b, the values undergo 4 obvious jumps within the given range, which suggests that 4 pairs of the non-rightmost roots are located in $(-0.002, 0.001) \times (-100\mathrm{i}, 100\mathrm{i})$, and their approximated values can be calculated from Step 3 of Algorithm 2 as $-0.000420 \pm 31.469\mathrm{i}$, $-0.000152 \pm 52.392\mathrm{i}$, $-0.0000775 \pm 73.327\mathrm{i}$, $-0.0000469 \pm 94.265\mathrm{i}$.

Example 4 Consider again a multi delay NDDE, for which the strong stability condition does not hold:

$$\dddot{x}(t) - \ddot{x}(t-\tau_1) + \ddot{x}(t-\tau_2) + \dot{x}(t) + x(t-\tau_3) + 50x(t) = 0\,. \tag{25}$$

The three-time delays are given as $\tau_1 = 2$, $\tau_2 = 3$, $\tau_3 = 1.5$, and the corresponding characteristic function reads as

$$f(\lambda) = \left(1 - \mathrm{e}^{-2\lambda} - \mathrm{e}^{-3\lambda}\right)\lambda^2 + \lambda + \mathrm{e}^{-1.5\lambda} + 50\,. \tag{26}$$

It can be seen that

$$\sup_{\Re(\lambda) > 0,\ |\lambda| \to \infty} \left|-\mathrm{e}^{-2\lambda} - \mathrm{e}^{-3\lambda}\right| = 2 > 1\,,$$

which suggests that the strong stability condition (3) does not hold. For such systems, though they might be stable when time delays are rationally dependent with each other, arbitrarily small perturbation could break this rationally dependence, and hence make the system unstable.

Similar to Example 2, the accumulation roots of Eq. (26) can be calculated by setting first coefficient to be zero, that is a two-delayed NDDE of the form

$$1 - \mathrm{e}^{-2\lambda} - \mathrm{e}^{-3\lambda} = 0. \tag{27}$$

Let $\lambda = \sigma + \omega\mathrm{i}$, Eq. (27) can be solved from

$$\begin{cases} 1 - \mathrm{e}^{-2\sigma}\cos(2\omega) - \mathrm{e}^{-3\sigma}\cos(3\omega) = 0 \\ \mathrm{e}^{-2\sigma}\sin(2\omega) + \mathrm{e}^{-3\sigma}\sin(3\omega) = 0 \end{cases},$$

which gives $\delta_1 \approx -0.141$ and $\delta_2 \approx 0.281$, and δ_2 determines the boundary between the rightmost roots and the non-rightmost roots.

The accumulation points can also be approximated by using the DIM. From Step 2 of Algorithm 2, the real part distribution of the roots in the square $(-1, 1) \times (-100\mathrm{i}, 100\mathrm{i})$ in the complex plane is obtained in Fig. 7a and b for both Eqs. (27) and (26).

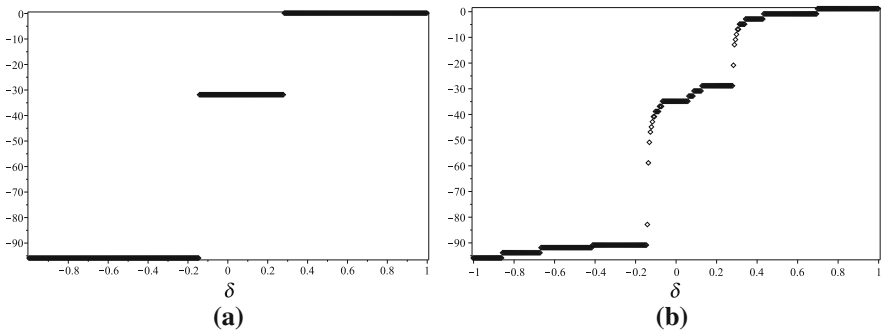

Fig. 7 Root jump with respect to $\delta \in (-1, -1)$ with $R = 100$ for **a**: Eq. (27) and **b**: Eq. (26)

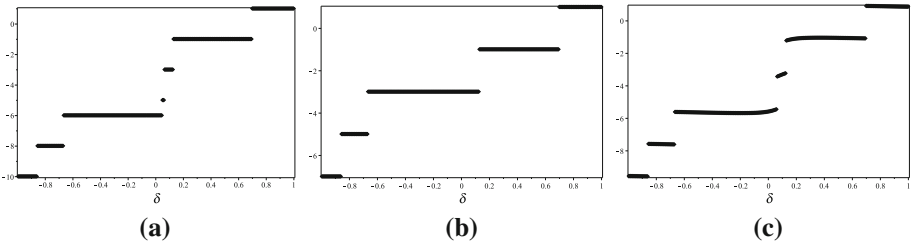

Fig. 8 Root jump of system (25) with respect to $\delta \in (-1, 1)$ for **a**: $R = 10$; **b**: $R = 8$; and **c** $R = 10$ without rounding off following Remark 8

As can be seen from both figures, the plotted value increases very rapidly at $\delta \approx -0.14$ and $\delta \approx 0.28$, which means that there are two accumulation points with real parts being close to these two values. Further calculation following Step 3 of Algorithm 2 gives the roots of Eq. (26) with similar real parts of the accumulation points, and a few of them are listed as follows: -0.113 ± 21.319i, -0.108 ± 22.695i, -0.127 ± 27.591i, -0.132 ± 33.869i, -0.125 ± 35.264i, -0.135 ± 40.149i, and that 0.341 ± 18.877i, 0.292 ± 43.992i, 0.290 ± 50.274i, 0.287 ± 56.556i, $0.286 + 62.839$i, 0.285 ± 69.121i.

In typical engineering problems, low frequency roots, i.e., the roots of small imaginary parts, are usually required. Thus Fig. 8a shows the plot for $R = 10$. Compared to $R = 100$ in Fig. 7b, the result in Fig. 8a needs less computational time because the integral interval is smaller. In Fig. 8a, the plotted value increases 2 by 5 times, and increases 1 by one time (at $\delta \approx 0.06$). Based on these jumping value, further iteration using Step 3 of Algorithm 2 calculates the corresponding 5 pairs of conjugates roots, giving -0.860 ± 1.546i, $-0.668 + 3.232$i, 0.128 ± 4.904i, 0.699 ± 6.942i, 0.065 ± 8.969i. However, the jumping at $\delta \approx 0.06$ should relate to a real root since the increment is only 1, which can easily be proved to be non-existent. Actually, from Remark 7, $\delta \approx 0.06$ corresponds to the situation when $\frac{F_{\delta_0^+}(0,R)}{\pi} = k + 1/2$, and by choosing a different $R = 8$, this false jumping can be avoided, as shown in Fig. 8b. Furthermore, from Remark 8, since $\frac{F_{\delta_0^+}(0,R)}{\pi} = k + 1/2$ introduces false jumping, we calculate only $F_\delta(0, R)/\pi$ with $R = 10$ for $\delta \in [-1, 1]$ as shown in Fig. 8c. The results show that the false jumping at $\delta \approx 0.06$ in Fig. 8a is avoided, and all other jumpings in Fig. 8c are related to the corresponding real parts of the characteristic roots of system (25) in $(-1, 1) \times (-10\text{i}, 10\text{i})$ of the complex plane.

5 Conclusion

This paper extends the DIM to calculate the characteristic roots of both retarded and neutral multi-delay systems with constant discrete delays. Based on the root shifting technique, the extended DIM first identifies the closely approximate real parts of the characteristic roots, and then calculates the imaginary parts by using the iteration method. Two algorithms are proposed to implement the extended DIM, both through capturing the changes in the number of the critical characteristic roots by shifting them on the complex plane. Among the two proposed algorithms, Algorithm 2 uses simpler criterion and is more recommended for use. Numerical examples show that the proposed method works efficiently and accurately.

The original DIM for stability test is derived and simplified from the Argument Principle. It holds the advantages of easy coding, high efficiency, as well as the ability of dealing with multiple time delays, and an increase in the number of delays does not pose particular difficulty in its implementation. Inheriting the merits of the original DIM, the extended DIM has simpler integrand and smaller integral interval, and hence improves the computational efficiency more. In addition, the extended DIM calculates all characteristic roots in an arbitrary and bounded area in the complex plane, regardless whether the strong stability condition holds or not. And a side benefit is that, since the real part distribution of the characteristic roots is calculated first, the extended DIM provides a fast way of estimating the rightmost roots and the accumulation point(s) by adjusting the upper limit of the integral, other than estimating them after calculating all the characteristic roots in the given region.

Supplementary Information The online version contains supplementary material available at https://doi.org/10.1007/s10915-021-01599-5.

Acknowledgements This work was supported by the Research Grant Council of the Hong Kong SAR under Grant PolyU 152036/18E, NSF of China under Grant 11702227, and the Fundamental Research Funds for the Central Universities under Grant A0920502051722.

Data Availibility Statement Data and material are available from the authors on reasonable request.

Declarations

Conflict of interest The authors declare that they have no competing financial interests.

Research Codes of the current study are available from the authors on reasonable request.

References

1. Zhang, S., Xu, J., Chung, K.: On the stability and multi-stability of a TCP/RED congestion control model with state-dependent delay and discontinuous marking function. Commun. Nonlinear Sci. Numer. Simul. **22**(1–3), 269–284 (2015)
2. Stepan, G.: Modelling nonlinear regenerative effects in metal cutting[J]. Philos. Trans. R. Soc. London A Math. Phys. Eng. Sci. **359**(1781), 739–757 (2001)
3. Li, Y., Tang, C., Peeta, S., et al.: Nonlinear consensus-based connected vehicle platoon control incorporating car-following interactions and heterogeneous time delays. IEEE Trans. Intel. Transp. Syst. **20**(6), 2209–2219 (2018)
4. Mukherjee, N.K., Shrira, V.: Intrinsic flame instabilities in combustors: analytic description of a 1-D resonator model. Combust. Flame **185**, 188–209 (2017)
5. Erneux, T.: Applied delay differential equations. Springer-Verlag, London (2009)

6. Du, Y., Niu, B., Guo, Y., et al.: Double Hopf bifurcation in delayed reaction-diffusion systems. J. Dyn. Differ. Equ., 2019: 1–46
7. Wernecke, H., Sandor, B., Gros, C.: Chaos in time delay systems, an educational review. Phys. Rep. **824**(3), 1–40 (2019)
8. Kuang, Y.: Delay Differential Equations with Applications to Population Dynamics. Academic Press, New York (1993)
9. Michiels, W., Niculescu, S.-I.: Stability and Stabilization of Time-Delay Systems (Advances in Design and Control). Society for Industrial and Applied Mathematics, Philadelphia (2007)
10. Pontryagin, L. S.: On the zeros of some elementary transcendental functions. Izvestiya Akademii Nauk. Seriya Matematicheskaya (Russian), 6(3), 115-134. English translation (1955) in American Mathematical Society Translations, 1942, 2, 95-110
11. Fu, M., Olbrot, A.W., Polis, M.: Robust stability for time-delay systems: the edge theorem and graphical tests. IEEE Trans. Autom. Control **34**(8), 813–820 (1989)
12. Fu, M., Olbrot, A.W., Polis, M.: The edge theorem and graphical tests for robust stability of neutral time-delay systems. Automatica **27**(4), 739–741 (1991)
13. Stepan, G.: Retarded dynamical systems: stability and characteristic functions. Longman Scientific & Technical Essex, 1989
14. Hassard, B.: Counting roots of the characteristic equation for linear delay-differential systems. J. Differ. Equ. **136**(2), 222–235 (1997)
15. Kolmanovskii, V., Myshkis, A.: Introduction to the theory and applications of functional differential equations. Kluwer Academic Publishers, Dordrecht (1999)
16. Xu, Q., Wang, Z.: Exact stability test of neutral delay differential equations via a rough estimation of the testing integral. Int. J. Dyn. Control **2**(2), 154–163 (2014)
17. Xu, Q., Stepan, G., Wang, Z.: Delay-dependent stability analysis by using delay-independent integral evaluation. Automatica **70**, 153–157 (2016)
18. Zhang, Q.F., Li, T.Y.: Asymptotic stability of compact and linear θ-methods for space fractional delay generalized diffusion equation. J. Sci. Comput. **81**(3), 2413–2446 (2019)
19. Wang, Z.H., Hu, H.Y.: Calculation of the rightmost characteristic root of retarded time-delay systems via Lambert W function. J. Sound Vib. **318**(4), 757–767 (2008)
20. Xu, Q., Stepan, G., Wang, Z.: Numerical stability test of linear time-delay systems of neutral type. Time Delay Systems. Springer, 2017, pp. 77-91
21. Hale, J.K., Lunel, S.M.V.: Strong stabilization of neutral functional differential equations. IMA J. Math. Control Inf. **19**(1 and 2), 5–23 (2002)
22. Engelborghs, K., Luzyanina, T., Samaey, G.: DDE-BIFTOOL: a Matlab package for bifurcation analysis of delay differential equations. TW Report 305, 2000
23. Barton, D.A., Krauskopf, B., Wilson, R.E., et al.: Collocation schemes for periodic solutions of neutral delay differential equations. J. Differ. Equ. Appl. **12**(11), 1087–1101 (2006)
24. Wang, Z.: Numerical Stability Test of Neutral Delay Differential Equations. Math. Problems Eng., 2008: 1–10
25. Vyhlidal, T., Zitek, P.: Quasipolynomial mapping based rootfinder for analysis of time delay systems. IFAC Proc. Vol. **36**(19), 227–232 (2003)
26. Vyhlidal, T., Zitek, P.: Mapping based algorithm for large-scale computation of quasi-polynomial zeros. IEEE Trans. Autom. Control **54**(1), 171–177 (2009)
27. Vyhlidal, T., Zitek, P.: QPmR-Quasi-polynomial root-finder: Algorithm update and examples, Delay Systems. Springer, 2014, pp. 299-312
28. Kyrychko, Y.N., Blyuss, K.B., Hovel, P., et al.: Asymptotic properties of the spectrum of neutral delay differential equations. Dyn. Syst. **24**(3), 361–372 (2009)

Publisher's Note Springer Nature remains neutral with regard to jurisdictional claims in published maps and institutional affiliations.